AEM00496-18
Revised draft
10-05-2018
Applied & Environmental Microbiology

Shuffling the neutral drift of unspecific peroxygenase in *Saccharomyces cerevisiae*

Javier Martin-Diaz[1], Carmen Paret[1], Eva García-Ruiz[2], Patricia Molina-Espeja[1] and Miguel Alcalde[1]*

[1]Department of Biocatalysis, Institute of Catalysis, CSIC, 28049 Madrid, Spain.

[2]Manchester Institute of Biotechnology, The University of Manchester, 131 Princess Street, Manchester M1 7DN, UK.

[*]Address correspondence to Miguel Alcalde: malcalde@icp.csic.es.

Key words: peroxygenases, neutral genetic drift, *in vivo* DNA shuffling, *Saccharomyces cerevisiae*, directed evolution.

Running title: peroxygenases by neutral drift and DNA shuffling.

ABSTRACT

Unspecific peroxygenase (UPO) is a highly promiscuous biocatalyst and its selective mono(per)oxygenase activity makes it useful for many synthetic chemistry applications. Among the broad repertory of library creation methods for directed enzyme evolution, genetic drift allows neutral mutations to be accumulated gradually within a polymorphic network of variants. In this study, we conducted a campaign of genetic drift with UPO in *Saccharomyces cerevisiae* so that neutral mutations were simply added and recombined *in vivo*. With low mutational loading and an activity threshold of 45% of the parent´s native function, mutant libraries enriched in folded and active UPO variants were generated. After only 8 rounds of genetic drift and DNA shuffling, we identified an ensemble of 25 neutrally evolved variants with modifications in peroxidative and peroxygenative activities, kinetic thermostability and enhanced tolerance to organic solvents. With an average 4.6 substitutions introduced per clone, neutral mutations covered roughly 10% of the protein sequence. As such, this study opens new avenues of UPO design by bringing together neutral genetic drift and DNA recombination *in vivo*.

IMPORTANCE

Fungal unspecific peroxygenase (UPO) resembles the peroxide shunt pathway of P450s to perform selective oxyfunctionalizations of unactivated C-H bonds with a broad range of organic compounds. In this study, we have combined neutral genetic drift and *in vivo* DNA shuffling to generate highly functional UPO mutant libraries. The panel of neutrally evolved UPOs showed different activity profiles for peroxygenative substrates and improved stability *vs*. temperature and the presence of organic co-solvents making them valuable blueprints for emergent evolution campaigns. This association of DNA recombination and neutral drift is paving the way for future works in UPO engineering, and from a more general perspective, to any other enzyme system heterologous expressed in *S. cerevisiae*.

INTRODUCTION

Fungal unspecific peroxygenase (UPO; EC 1.11.2.1) is a new class of extracellular heme-thiolate peroxidase with exclusive mono(per)oxygenase activity that is attracting the attention of the biotechnology community (1,2). With a wide substrate promiscuity, this highly selective and stable biocatalyst inserts oxygen into unactivated C-H bonds at room temperature, and at atmospheric pressure, what represented a mere pipedream to synthetic chemists only a few years ago. Taking advantage of the peroxide shunt pathway of classic P450 monoxygenases, UPO can behave as a self-sufficient monooxygenase triggered by H_2O_2, which acts as the final electron acceptor and main oxygen source (3). The spectrum of oxyfunctionalization reactions covered by UPO includes brominations, sulfoxidations, N-oxidations, aromatic hydroxylations, alkyl hydroxylations, epoxidations and ether cleavage, which makes us optimistic about the forthcoming applications of this enzyme as an industrial biocatalyst (4). This is especially true, if UPO is compared with the well-studied P450s, whose dependence on expensive redox co-factors and auxiliary flavoproteins, together with the oxygen dilemma associated with the production of unproductive oxygen species and its poor stability, has prevented them from becoming the natural replacement of chemical catalysts in dozens of consolidated industrial reactions (5).

In terms of the industrial use of UPO, one of the main issues that remains pending is its oxidative inactivation by H_2O_2, which is currently being tackled by developing sophisticated *in situ* H_2O_2 supply systems. Such approaches conceptually unify the fields of chemical catalysis, photocatalysis and biocatalysis, with the aim of updating long-standing industrial processes through the inclusion of ad-hoc engineered, efficient and stable UPO variants (6-8). In this regard, advances in UPO design have recently been achieved through directed evolution, addressing aspects from its heterologous functional expression in yeast to the synthesis of chemicals and

pharma compounds (9-14). These evolutionary enterprises have been carried out by adaptive evolution, *i.e.* the construction and exploration of mutant libraries to find the best suited clones according to well-defined selection criterion (15,16). Unlike traditional adaptive evolution, where screening efforts focus on the selection of the fittest, directed evolution by neutral genetic drift pursues the gradual accumulation of neutral mutations within a population of variants with similar phenotypes but different genotypes (17). Conversely, iterative rounds of random mutation coupled to a selective pressure to maintain the native enzyme function produce polymorphic networks enriched in functional mutants, while detrimental mutations are purged in a process also referred to as “purifying selection” (18). Neutral drift is commonly used to unmask hidden properties, such as latent/promiscuous activities and stability, as demonstrated in studies on P450s, lactonases, β-lactamases, phosphotriesterases, polysialyltransferases and β-glucuronidases, among other examples (19-27). However, the accumulation of neutral mutations is not straightforward, in part because the activity cut-off employed to maintain the wild-type function favors contamination of the clones selected with parental sequences. Given that ~45% of mutant libraries generated by low mutational loading is waste, mostly due to the presence of the parental type (28), the search of neutral variants by genetic drift requires substantial experimental input unless ultrahigh-throughput screening or genetic selection procedures are available. Indeed, the average number of generations in a campaign of neutral drift ranges from ~15 to 25 (16,17,29). Although the potential to use DNA recombination in genetic drift experiments has long been suggested, all the studies reported to date have lacked an efficient recombination system that enables neutral mutations to be simultaneously recombined between homologues in each round of neutral evolution.

In the current work, we have prepared a genetic drift protocol that allows neutral mutations to be introduced in conjunction with simultaneous *in vivo* recombination. The “drifted” UPO libraries expressed in *Saccharomyces cerevisiae* were analyzed in terms

of their substrate promiscuity as well as their stability against temperature and the presence of organic solvents. An ensemble of 25 neutral homologues were subjected to a preliminary characterization, and the most promising variants were purified to homogeneity and studied biochemically.

MATERIALS AND METHODS

Materials

Agrocybe aegerita UPO secretion mutant (PaDa-I) was obtained as described elsewhere (9). Expression shuttle vector pJRoC30 containing an uracil auxotrophy and ampicillin marker for selection came from California Institute of Technology (CALTECH, USA). ABTS (2,2'-azino-bis(3-ethylbenzothiazoline-6-sulfonic acid)), DMP (2, 6-dimethoxyphenol), veratryl alcohol, benzyl alcohol, Tween20, hemoglobin from bovine blood, ascorbic acid, anthracene, *Taq* DNA polymerase and Yeast transformation kit were purchased from Sigma-Aldrich (Madrid, Spain). NBD (5-nitro-1,3-benzodioxole) was acquired from TCI America (Portland, OR, USA). Naphthalene and DL-propranolol hydrochloride was obtained from Acros Organics (Geel, Belgium). *S. cerevisiae* strain BJ5465 was from LGC Promochem (Barcelona, Spain) while *Escherichia coli* XL2-Blue competent cells were from Stratagene (La Jolla, CA, USA). Zymoprep yeast plasmid miniprep kit and Zymoclean Gel DNA Recovery Kit were from Zymo Research (Orange, CA, USA). The NucleoSpin plasmid kit was purchased from Macherey-Nagel (Düren, Germany). The restriction enzymes BamHI and XhoI were from New England Biolabs (Hertfordshire, UK). Oligonucleotides were synthesized by Metabion (Bayern, Germany). All chemicals were reagent-grade purity.

Culture media

Minimal medium, SC drop-out plates and Luria-Bertani (LB) medium were prepared as reported elsewhere (9). Selective expression medium (SEM) contained 100 mL 6.7% filtered yeast nitrogen base, 100 mL 19.2 g/L filtered yeast synthetic

drop-out medium without uracil, 100 mL 20% filtered galactose, 67 mL 1 M filtered KH_2PO_4 pH 6.0 buffer, 22 mL filtered $MgSO_4$ 0.1 M, 34.8 mL absolute ethanol, 1 mL 25 g/L filtered chloramphenicol and $_{dd}H_2O$ up to 1 L. Hemoglobin expression medium included 712.5 mL YP 1.55X, 66 mL 1 M filtered KH_2PO_4 pH 6.0 buffer, 110 mL 20% filtered galactose, 22 mL filtered $MgSO_4$, 31.5 mL absolute ethanol, 16.5 mL 20g/L filtered hemoglobin, 1.1 mL 25 g/L filtered chloramphenicol and $_{dd}H_2O$ up to 1 L.

Mutant library creation

Eight rounds of neutral drift and DNA shuffling were performed. pJRoC30 was linearized with BamHI and XhoI. Linearized vector was cleaned, concentrated and loaded onto a low melting-point preparative agarose gel and purified using the Zymoclean Gel DNA Recovery Kit.

Error-Prone PCR (epPCR): Except for the first round of neutral drift (where PaDa-I was the parental type), the collection of plasmids satisfying the activity threshold (see below) was subjected to epPCR with *Taq* DNA polymerase in presence of $MnCl_2$ (mutational load: 1 to 3 mutations/Kb). Primers used for amplifications were: RMLN sense (5´-CCTCTATACTTTAACGTCAAGG-3´) and RMLC antisense (5´-GGGAGGGCGTGAATGTAAGC -3´). The epPCR was carried out in 50 µL of final volume containing 3% dimethyl sulfoxide (DMSO), 90 nM RMLN, 90 nM RMLC, 0.3 mM deoxynucleoside triphosphates (dNTPs) (0.075 each), 0.01 mM $MnCl_2$, 1.5 mM $MgCl_2$, 0.05 U/µL *Taq* DNA polymerase and 0.14 ng/µL of the corresponding templates. epPCR was performed on a gradient thermocycler (Mycycler, BioRad, USA) using the following parameters: 95ºC for 2 min (1 cycle); 94ºC for 45 s, 55ºC for 30 s, 74ºC for 90 s (28 cycles); and 74ºC for 10 min (1 cycle). PCR product was purified using the Zymoclean Gel DNA Recovery Kit.

In vivo DNA shuffling: 200 ng of epPCR product were mixed with 100 ng of the linearized vector and transformed into *S. cerevisiae* competent cells using the Yeast transformation kit. Inserts and linearized plasmid shared 50 bp of homology to allow

recombination and the *in vivo* cloning by the yeast. Transformed cells were plated on SC drop-out plates being incubated for 3 days at 30ºC.

High-throughput screening

Individual colonies were picked and cultured in 96-well plates containing 210 µL of SEM per well. In each plate, column 6 was inoculated with parental PaDa-I mutant and well-H1 (containing minimal medium supplemented with uracil) was inoculated with untransformed *S. cerevisiae* as a negative control. Plates were incubated at 30ºC, 230 rpm and 80% relative humidity (Minitron-INFORS, Switzerland). After 72 h, plates were centrifuged (Eppendorf 5810R centrifuge, Germany) for 10 min at 3500 rpm and 4ºC. 20 µL of supernatant were transferred to new plates by a robotic liquid handling station (Freedom EVO 100 base, TECAN Schweiz AG, Switzerland). 180 µL of a reaction mixture (100 mM sodium phosphate/citrate buffer pH 4.4, 0.3 mM ABTS and 2 mM H_2O_2) were added to each plate with the help of a pipetting robot (Multidrop Combi Reagent Dispenser, Thermo Scientific, USA). The plates were briefly stirred measuring the absorbance at 418 nm ($\varepsilon_{ABTS^{\cdot+}}$ = 36,000 M^{-1} cm^{-1}) in kinetic mode with a plate reader (SPECTRAMax Plus 384, Molecular Devices, USA). The obtained values were normalized against the corresponding parental type in each plate (9).

Purifying selection: The cut-off for UPO activity was set at 45% of parental´s activity (clones with activity below that threshold were purged). Using the high-throughput screening described above, the selected clones (20 µl each from re-suspended cell pellets) were pooled together and subjected to plasmid extraction using the Zymoprep yeast plasmid miniprep. To remove impurities and enhance the yield, the resulting mixed DNA product was transformed into *E. coli* XL2-Blue cells, plated in a LB-amp agar plate and grown at 37ºC overnight. Transformed colonies were scratched from the LB-plate and inoculated in 2 mL LB. Mutant library plasmid extraction was performed using the NucleoSpin plasmid kit. Purified mixture was used as template for a new round of epPCR and DNA shuffling as described above.

186 **Production of neutral variants**

187 For each selected neutral clone, cell pellets were re-suspended by pipetting up
188 and down and stirring. 20 µL of re-suspended mixture was transferred to 3 mL of
189 minimal medium. After 48 h at 30ºC and 220 rpm, plasmids were extracted by
190 Zymoprep. *E.coli* XL2-Blue were transformed with the Zymoprep product, plated into
191 LB-amp agar plates and grown at overnight at 37ºC. Single colonies were inoculated in
192 5 mL LB-amp medium and were grown at 37ºC overnight. Plasmids were extracted,
193 transformed into *S. cerevisiae* cells and plated on SC drop-out plates. After 3 days at
194 30ºC, single colonies were inoculated in 5 mL of minimal medium and incubated for 48
195 h at 30ºC and 220 rpm. Clones were refreshed in a final volume of 5 mL minimal
196 medium with an optical density OD_{600} = 0.3. After 6-8 h of growing (OD_{600}=1-1.5), 9 mL
197 of hemoglobin expression medium were inoculated with 1 mL pre-culture and
198 incubated 48h at 30ºC and 250 rpm in a 100 mL flask. Growth and expression were
199 followed by measuring the OD_{600} of the cultures and the activity against ABTS, as
200 described below, until reaching the stationary phase. Cells were removed by
201 centrifugation at 3500 rpm and 4ºC during 15 min, saving the supernatant for the
202 activity and stability assays.

203 **Activity and stability assays**

204 ABTS: 20 µL of supernatant were mixed with 180 µL of 100 mM sodium
205 phosphate/citrate buffer pH 4.4, 0.3 mM ABTS and 2 mM H_2O_2. The plates were briefly
206 stirred and the absorbance was measured at 418 nm (ε_{418}=36,000 $M^{-1}\,cm^{-1}$) (9).

207 NBD: 20 µL of supernatant were mixed with 180 µL of 100 mM sodium phosphate
208 buffer pH 7.0 containing 1 mM NBD (15% final concentration of acetonitrile) and 1 mM
209 H_2O_2. The plates were briefly stirred and the absorbance was measured at 425 nm
210 (ε_{425}=9,700 $M^{-1}\,cm^{-1}$) (9).

Naphthalene: 20 µL of supernatant were mixed with 180 µL of 100 mM potassium phosphate buffer pH 7.0 containing 0.5 mM of naphthalene (10% final concentration of acetonitrile) and 1 mM of H_2O_2. After a reaction time of 10 min, 20 µL of Fast Red [Fast Red TR Salt hemi(zinc chloride salt)] were added to each well and plates were incubated at room temperature until a red color developed. The absorption was measured at 510 nm (ε_{510}=4,700 M^{-1} cm^{-1}) (11).

Propranolol: 40 µL of supernatant were mixed with 180 µL of 100 mM sodium phosphate buffer pH 7.0 containing 5 mM propranolol, 2 mM H_2O_2 and 4 mM of ascorbic acid. After a reaction time of 60 min, the sample was subjected to the 4 aminoantipyrine (4-AAP) assay with minor modifications (14). Plates were stirred briefly and absorption at 530 nm was recorded.

Anthracene: 400 µL of supernatant were mixed with 600 µL of 20 mM potassium phosphate buffer pH 7.0 containing 1mM of anthracene (20% final concentration of acetonitrile), 1% of Tween20 and 1 mM of H_2O_2. After 1 h, reactions were stopped incubating 10 min at 90ºC. Activities were analyzed by reversed-phase high-performance liquid chromatography (HPLC) with equipment consisting of a tertiary pump (Varian/Agilent Technologies, USA) coupled to an autosampler (Merck Millipore, USA) and an ACE C18 PFP (pentafluorophenyl, 15 cm x 4.6 mm) column at 40ºC. Detection was performed with a PDA (Variant/Agilent Technologies, USA) at 355 nm. The mobile phase was methanol (80%) and *dd*H_2O (20%) at a flow rate of 0.8 mL min^{-1}.

Activity in organic solvents: The relative activities in organic solvents were assessed following the ABTS assay described above (100 mM sodium phosphate/citrate buffer pH 4.4, 0.3 mM ABTS and 2 mM H_2O_2) supplementing the reaction mix with the corresponding concentration of organic solvent (12% acetonitrile; 6% DMSO, 3% ethanol) and appropriate dilutions of supernatants. Tolerance in organic solvent (*i.e.* retained activity in co-solvents) is defined as the ratio of the activity in the presence of

organic solvents to that in the absence of organic solvents, expressed in folds *vs*. parental type.

Kinetic thermostability (T_{50}): Appropriate dilutions of supernatants were prepared in 10 mM potassium phosphate buffer pH 7.0 such a way that aliquots of 20 µL gave rise to a linear response in kinetic mode. 50 µL supernatant were used for each point in a gradient scale ranging from 30 to 80°C. This gradient profile was achieved using a thermocycler. After 10 min of incubation, samples were removed and chilled out on ice for 10 min. After that, samples of 20 µL were removed and incubated at room temperature for 5 min. Finally, samples were subjected to the same ABTS colorimetric assay described above for the screening (100 mM sodium phosphate/citrate buffer pH 4.4, 0.3 mM ABTS and 2 mM H_2O_2). Thermostability values were calculated from the ratio between the residual activities incubated at different temperature points and the initial activity at room temperature. The T_{50} value was determined by the transition midpoint of the inactivation curve of the protein as a function of temperature, which in our case was defined as the temperature at which the enzyme lost 50% of its activity following an incubation of 10 minutes.

Purification

Mutants 6.1, 4.7, 7.1, 16.5 and PaDa-I were produced and purified to homogeneity. A single *S. cerevisiae* colony from each variant was inoculated in 20 mL of minimal medium and incubated for 48 h at 30ºC and 230 rpm. Clones were refreshed in a final volume of 250 mL minimal medium at an optical density OD_{600} = 0.3. After 6-8 h of growing (OD_{600}=1-1.5), 900 ml of hemoglobin expression medium were inoculated with 100 mL pre-culture and grown 72h at 25ºC and 250 rpm. Expression was followed by measuring the OD_{600} of the cultures and the activity against ABTS, as described above, until reaching the stationary phase. Cells were removed by centrifugation at 6000 rpm and 4ºC during 30 min saving the supernatants for enzyme assays. Supernatants were filtered using a nitrocellulose membrane of 0.45 µm pore size. Then, supernatants

were concentrated using a Pellicon tangential ultrafiltration system (10 kDa cut-off membrane; Millipore, USA) and an Amicon stirred ultrafiltration cell (10 kDa cut-off membrane; Millipore, USA), followed by dialysis against 20 mM sodium citrate pH 3.3 buffer (buffer A). The samples were filtered and loaded into two cation-exchange HiTrap SP FF columns in a row connected to an ÄKTA purifier system (GE Healthcare, UK) and pre-equilibrated with buffer A. The proteins were eluted with a linear gradient from 0 to 40% in 60 min of buffer A containing 1M NaCl. Fractions with ABTS activity were collected, concentrated and dialyzed against 20 mM Tris-HCl pH 7.8 buffer (buffer B) and loaded into a BioSuite Q anion-exchange column (Waters, USA), pre-equilibrated with buffer B. Proteins were eluted with a linear gradient from 0 to 20% in 40 min of buffer B containing 1M NaCl. The fractions with UPO activity towards ABTS were collected and dialyzed against 10 mM potassium phosphate pH 7.0 buffer. Samples of pure enzymes were stored at 4ºC. The Reinheitszahl values [R_Z] [A_{418}/A_{280}] achieved were ~2. Throughout the purification protocol, the fractions were analysed by SDS/PAGE on 12% gels and the proteins were stained with SeeBand Protein Staining solution (Gene Bio-Application Ltd, Israel). The concentrations of all crude protein extracts were determined using the Bio-Rad protein reagent and BSA as standard.

Biochemical characterization of purified neutral variants

Kinetic parameters: Kinetic values were estimated with increasing substrate concentrations and fitted to a single rectangular hyperbola function by Michaelis-Menten model with the use of SigmaPlot 10.0, where parameter *a* was equal to k_{cat} and parameter *b* was equal to $K_{m.}$ Kinetics for ABTS were measured in 100 mM sodium citrate/phosphate buffer pH 4.0 containing 2 mM of H_2O_2. Kinetics for NBD were performed in 100 mM potassium phosphate buffer pH 7.0 containing 1 mM of H_2O_2 in 15% of acetonitrile. Kinetics for DMP were carried out in potassium phosphate buffer pH 7.0 and 2 mM of H_2O_2. Kinetics for naphthalene were performed in 100 mM potassium phosphate buffer pH 7.0 containing 1 mM of H_2O_2 in 20% of acetonitrile.

Propranolol kinetics were assayed in potassium phosphate buffer pH 7.0 containing 2 mM of H_2O_2 and 4 mM of ascorbic acid. Kinetics for benzyl alcohol were performed in potassium phosphate buffer pH 7.0 containing 2 mM of H_2O_2. Kinetics for veratryl alcohol were carried out in potassium phosphate buffer pH 7.0 containing 2 mM of H_2O_2. For each substrate, reactions were performed by triplicate following the increase of the absorption for ABTS (ε_{418}=36,000 M^{-1} cm^{-1}); NBD (ε_{425}=9,700 M^{-1} cm^{-1}); DMP (ε_{469}=27,500 M^{-1} cm^{-1}); propranolol (ε_{325}=1,996 M^{-1} cm^{-1}) naphthalene (ε_{303}=2,010 M^{-1} cm^{-1}); benzyl alcohol (ε_{280}=1,400 M^{-1} cm^{-1}) and veratryl alcohol (ε_{310}=9,300 M^{-1} cm^{-1}).

Determination of C_{50}: Activity in organic solvents was assessed in kinetic mode using the ABTS assay described above (100 mM sodium phosphate/citrate buffer pH 4.4, 0.3 mM ABTS and 2 mM H_2O_2) containing the corresponding concentration of co-solvent and appropriate dilutions of enzymes. The C_{50} was defined as the concentration of co-solvent (expressed in % (v/v)) at which the enzyme shows 50% of the corresponding activity in buffer.

Determination of $t_{1/2}$: Appropriate dilutions of enzymes in 10 mM potassium phosphate buffer pH 7.0 were incubated at 63ºC. Every 5 min, aliquots of 20 µL were removed and residual activity was determined in kinetic mode following the ABTS assay described above (100 mM sodium phosphate/citrate buffer pH 4.4, 0.3 mM ABTS and 2 mM H_2O_2). The half-life ($t_{1/2}$) was defined as the time required by the enzyme - after incubation at 63ºC- to lose 50 % of its initial activity at room temperature.

DNA sequencing

UPO genes were sequenced by GATC-Biotech. The primers used were: RMLN, apo1secdir (5´-GAGCCAGGATTACCTCCTG-3´), apo1secrev (5´-GGTCATACTGGCGTCGCCTTC-3´) and RMLC.

316 **Protein modeling**

317 The mutations introduced by neutral genetic drift were mapped using the crystal
318 structure of native UPO from *A. aegerita* at a resolution of 2.1 Å (protein Data Bank
319 Europe [PDB] accession number 2YOR) (30). The model was generated and analyzed
320 by PyMOL Molecular Visualization System (http:// pymol.org).

321 **RESULTS AND DISCUSSION**

322 **1. Departure point and protocol for shuffling drifted libraries in *S. cerevisiae***

323 As the point of departure for this study, we used a secretion mutant evolved
324 from *Agrocybe aegerita* UPO for its heterologous functional expression in yeasts,
325 PaDa-I. This variant harbours nine mutations that yield abundant expression in *S.*
326 *cerevisiae* and *Pichia pastoris*: F12Y-A14V-R15G-A21D-V57A-L67F-V75I-I248V-
327 F311L (underlined mutations lie in the signal peptide) (9,10). Performing directed
328 evolution in *S. cerevisiae* offers many advantages in terms of library creation (31,32).
329 Given its high frequency of homologous DNA recombination, transformed genes with
330 identities as low as 50% are rapidly shuffled *in vivo* without the need for cleavage sites
331 or DNases. Thus, to set out the genetic drift campaign, we wired each round of random
332 mutation to *in vivo* DNA shuffling by designing 50 bp flanking overhangs between the N
333 and C terminals of the epPCR products and the linearized vector (**Fig. 1**). Using this
334 strategy, neutral, unfragmented homologues were freely recombined, whereas the full
335 autonomously replicating plasmid was repaired in just a single transformation step. A
336 mutational load of 1-3 substitutions per Kb was chosen, as higher mutation frequencies
337 would augment the number of inactive clones and jeopardize the diversity in the drifted
338 library.

339 Although the evolutionary lineage for natural UPO remains unclear, the
340 convergence of peroxidative activity (one electron oxidation reactions) and
341 peroxygenative activity (O-transfer by two electron oxidations) within the same enzyme

provides insight into its original native function. Considering UPO as the first truly natural peroxygenase implies that this enzyme is the missing catalytic link between heme-thiolate enzymes and classic peroxidases (3). The hybrid catalytic mechanism employed by UPO suggests that peroxygenative activity could plausibly have evolved from an ancestral peroxidative activity. Accordingly, to maintain the protein´s original function and structure, while gradually accumulating neutral mutations, we imposed the constraint that UPO variants had to oxidize a peroxidative substrate and exceed a threshold of 45% of the parental activity. This activity threshold represented a compromise between improved stability and the exploration of promiscuous activities. Indeed, stringent cut-offs (~75%) are used to improve stability whereas more relaxed ones (~30%) are established for latent activities (17). Given that the physiological function of UPO is still unknown (among the possible roles in nature have been proposed the synthesis of metabolites, detoxification processes and humus and lignin degradation), we chose ABTS as surrogate peroxidative substrate during purifying selection. ABTS is commonly used to screen heme-containing peroxidase libraries, and it offers excellent sensitivity limits, low coefficient of variance and low interactions with the yeast culture broth (9).

2. Neutral drift campaign

Under the aforementioned premises, the PaDa-I variant was submitted to 8 rounds of neutral drift combined with *in vivo* shuffling. Although the same mutational load was maintained throughout the entire genetic drift experiment, the percentage of neutral clones selected that conformed to the activity threshold in each round fluctuated slightly as a consequence of the recombination in yeast and the gradual accumulation of neutral mutations (with 45% and 30% of functional clones in rounds 1 and 8, respectively, (**Fig. 2**)). In the third generation, we established a mid-check point of the drifted library by selecting 30 neutral clones at random (using Python software, a random number generator). We first monitored the accumulation of mutations by

sequencing the selected variants. Of the 30 clones, 13 incorporated amino acid substitutions in the mature UPO, with an average mutational rate of 2.4 nucleotide mutations per clone. In addition, 12 clones contained only silent mutations that may have an important role in future adaptation processes and 5 clones were of the parental type. The 13 neutral variants with amino acid substitutions were produced and subjected to a preliminary characterization. The majority of the mutations were situated at the surface of the protein, far from the relevant catalytic sites (**Fig. S1** in the supplemental material). When kinetic thermostability was estimated by measuring the T_{50} of the variants (the temperature at which the enzyme lost 50% of its activity after a 10 min incubation), 3 mutants showed a ~2 ºC improvement over the parental enzyme (clone 4, V298A; clone 33, K302Q; and clone 39, V247A, (**Fig. S2A** in the supplemental material). In terms of activity, the initial turnover rates for ABTS, DMP (peroxidative substrates), NBD and napthalene (peroxygenative substrates) were assessed, detecting some mild deviations (*e.g.* the activity of variant 4 on ABTS, DMP and NBD improved around 1.5-fold; (**Fig. S2B** in the supplemental material). In the light of these data, we moved forward with the neutral drift/DNA shuffling campaign until completing 8 rounds (~7,000 clones screened).

Of the 191 neutral clones obtained in generation 8, 25 were produced and their culture supernatants used for a preliminary characterization. The broad sequence diversity of these neutrally evolved homologues was evident in the phylogenetic trees derived from nucleotide and amino acid substitution, (**Fig. 3**). On average, we identified 4.6 nucleotide mutations per clone (115 mutations in total) of which 40 were non-synonymous mutations over 27 positions, almost 10% of the protein sequence, (**Table S1** in the supplemental material). 80% of mutations were situated at the surface of the protein and only two in the catalytic center (**Fig. 4**) whereas we found a 25% enrichment in mutations (*i.e.* appearing in more than one sequence). It is highly likely that many of the enriched mutations were actually consensus-ancestor mutations as also described in other neutral drift campaigns (22), given their location (the majority of

them at the surface of the protein structure, far from the catalytic pocket) and their thermostabilizing effects; however, the influence of DNA recombination on such enrichment cannot be ruled out either. Unfortunately, UPO is a relatively novel protein and the lack of sufficient reliable sequences (to date, there are only four UPOs characterized from *Agrocybe aegerita* (33), *Coprinellus radians* (34), *Marasmius rotula* (35) and *Chaetomium globosum* (36)) hampered us to perform a solid multiple sequence alignment to unveil the possible consensus-ancestor origin of neutral mutations. The increasing number of hypothetical UPO sequences deposited in genomic databases along with the efforts done by my lab and others in expressing new UPO sequences will pave the way to apply consensus design and phylogenetic analysis aimed at finding stabilizing ancestor/consensus mutations or even resurrecting ancestral nodes of UPO proteins in the near future (12).

The substrate promiscuity of the neutral variants was first analyzed with a panel of peroxygenative substrates, including NBD, propranolol, anthracene, naphthalene, as well as with the peroxidative ABTS. A heat map enabled the neutral variants to be arranged into hierarchical clusters according to the improved activity on all 5 substrates relative to the neutral evolution parental PaDa-I, (**Fig. 5A**). The fold change in activity as the ratio of the variant´s activity for each substrate to that of the parental PaDa-I allowed us to easily sort the neutral variants according to their activity preferences while helping to discriminate among possible secretion mutants. The lack of correlation between the activities for the 5 substrates addressed the absence of secretion mutants within the set of neutral clones analyzed, which was confirmed by SDS-PAGE analysis, (**Fig. S3** in the supplemental material). There was a modest increase or decrease in the oxidation of ABTS in the majority of the neutral variants, although all retained at least 45% of the activity of PaDa-I (the minimum requirement for selection). The average improvement/reduction ratio of neutral variants to oxidize ABTS was close to the activity of PaDa-I (0.95±0.3). By contrast, there were more pronounced changes in

the latent activities for peroxygenative substrates than those detected for ABTS. For example, many of the variants had a ~2-fold improved activity for the dealkylation of NBD with the order of preference for the oxidation of peroxygenative substrates as follows: NBD>propranolol>anthracene>naphthalene. The robustness of the variants in terms of high temperature tolerance and that of organic solvents was also monitored and as evident with substrate preference, substantial changes were detected although a clear relationship between thermostability and tolerance to co-solvents could not be established, (**Fig. 5B**). Roughly half of the variants had improved thermostability, while the resistance to co-solvents mostly followed the pattern DMSO>acetonitrile (ACN)>ethanol.

3. Biochemical characterization of purified neutral variants

To inspect the changes detected in stability and activity in more detail, several neutral variants (6.1 [F191L-S226G-Q254R], 7.1 [G119S], 4.7 [S272P-A317D] and 16.5 [L88P-Q249R-Q254R]) were produced on a larger scale and purified to homogeneity (Reinheitszahl value [R_Z] [A_{418}/A_{280}] ~ 2), (**Fig S4A-C** in the supplemental material). In terms of stability, the 16.5 variant was more thermostable, improving the half-life ($t_{1/2}$) of the parental PaDa-I by 34 min, while the 6.1 variant duplicated the parental type value ($t_{1/2}$ was defined as the time required to lose 50 % of activity after incubating the enzyme at 65 ºC, (**Table 1**, **Fig. S5A** in supplemental material). Strikingly, both the 6.1 and 4.7 variants notably increased their tolerance to organic solvents, especially against ACN, with C_{50} values of ~20% as opposed to the 7% of the parental PaDa-I (the C_{50} was defined as the concentration of co-solvent -expressed as a % (v/v)- at which the enzyme losses half of its corresponding activity, (**Table 1, Fig. S5B-D** in supplemental material). This tolerance was also evident to a lesser extent for acetone, methanol and DMSO but not for ethanol. The kinetic parameters of the variants were assessed with a panel of peroxidative (ABTS, DMP) and peroxygenative (veratryl alcohol, benzyl alcohol, NBD, naphthalene and propranolol) substrates,

(**Table 2**). The peroxygenative:peroxidative ratio (*P:p* ratio) plays a key role on the aromatic hydroxylation reactions performed by UPO: the products of the peroxygenative activity on aromatics (phenolics) become peroxidative substrates, thereby being oxidized by UPO into phenoxyl radicals jeopardizing the final reaction yields. Some of the neutrally evolved variants of our study showed slight modifications in the *P:p* ratio that were dependent on the substrate tested. In this regard, recent findings (11, 13, 14 and unpublished material) address that the *P:p* ratio is mostly reliant on the nature of the targeted substrates, which defines the access to the heme channel and the residence time at the binding site for a proper oxygenation/oxidation, rather than from the existence of catalytic radical forming residues at the protein surface to work through a long range electron transfer pathway to the heme, as described for ligninolytic peroxidases (38). The variants with the strongest thermostabilities (16.5, 6.1) displayed an overall decrease in catalytic efficiencies (k_{cat}/K_m), which may be connected to a putative trade-off between activity and stability that can be circumvented by different engineering strategies (39 and references herein). The most notable improvements in activity were detected for the variants 7.1 and 4.7, and while there was an enhancement of up to ~1.5-fold in the k_{cat}/K_m of 7.1 for NBD, naphthalene and DMP, variant 4.7 had an 1.7- and 1.5-fold enhanced catalytic efficiency for NBD and propranolol, respectively. The latter is of special pharmaceutical interest since this compound is a widely used beta-blocker that UPO can convert into the equipotent human drug metabolite 5-OH´-propranolol (14).

CONCLUSIONS

Neutral genetic drift is a powerful tool to modify the substrate promiscuity and stability of enzymes, whereas DNA shuffling is a long-established recombination method to unify beneficial mutations from different parents and/or to purge detrimental ones. In this work, we describe a “one-pot” approach that brings together genetic drift and DNA shuffling in *S. cerevisiae* in order to generate highly functional UPO libraries.

Indeed, the accumulation of neutral mutations and their simultaneous recombination *in vivo* helped speed up the genetic drift process, while removing destabilizing mutations in a drive towards more evolvable drifted libraries. The less stringent activity threshold established during screening allowed both the stability and activity of the UPO variants to be controlled. Given that many of the industrial reactions that UPO can perform take place under harsh conditions, some of the neutrally evolved UPOs from this study represent a promising departure point for further engineering towards stronger tolerance to co-solvents or higher thermostabilities. Moreover, some modifications found in the palette of activities, such as transformation to the promiscuous substrate propranolol, open up avenues to design highly efficient UPO variants for the synthesis of human drug metabolites, important compounds in pharmacokinetic and pharmacodynamics studies.

ACKNOWLEDGEMENTS

This work was supported by the European Union [FP7-KBBE-2013-7-613549-INDOX; H2020-BBI-PPP-2015-2-720297-ENZOX2], the CSIC [project PIE-201580E042], and the Spanish Ministry of Economy, Industry and Competitiveness [projects BIO2013-43407-R.DEWRY and BIO2016-79106-R. LIGNOLUTION].

REFERENCES

1. Bormann S, Gomez-Baraibar A, Ni Y, Holtmann D, Hollmann F. 2015. Specific oxyfunctionalizations catalyzed by peroxygenases: opportunities, challenges and solutions. Catal Sci Technol 5:2038-2052.
2. Wang Y, Lan D, Durrani R, Hollmann F. 2017. Peroxygenases en route to becoming dream catalysts. What are the opportunities and challenges?. Curr Opin Chem Biol 37:1-9
3. Hofrichter M, Kellner H, Pecyna MJ, Ullrich R. 2015. Fungal unspecific peroxygenases: Heme-thiolate proteins that combine peroxidase and cytochrome P450 properties, p 341-368. *In* Hrycay EG, Bandiera SM. (ed),

505 Monooxygenase, Peroxidase and Peroxygenase Properties and Mechanisms of
506 Cytochrome P450, vol 851. Adv Exp Med Biol, USA.

507 4. Hofrichter M, Ullrich R. 2013. Oxidations catalyzed by fungal peroxygenases.
508 Curr Opin Chem 19:116-125.

509 5. Holtmann D, Hollmann F. 2016. The oxygen dilemma: a severe challenge for
510 the application of monooxygenases. ChemBioChem 17:1391-1398.

511 6. Ni Y, Fernandez-Fueyo E, Gomez-Baraibar A, Ullrich R, Hofrichter M, Yanase
512 H, Alcalde M, van Berkel WJH, Hollman F. 2016. Peroxygenase-catalysed
513 oxyfunctionalization reactions promoted by the complete oxidation of methanol.
514 Angew Chem Int Edit 55: 798-801.

515 7. Zhang W, Burek BO, Fernandez-Fueyo E, Alcalde M, Bloh JZ, Hollmann F.
516 2017. Selective activation of C-H bonds by cascading photochemistry with
517 biocatalysis. Angew Chem Int Edit 56:15451-15455.

518 8. Zhang W, Fernandez-Fueyo E, Ni Y, van Schie M, Gacs J, Renirie R, Wever R,
519 Mutti FG, Rother D, Alcalde M, Hollmann F. 2018. Selective aerobic oxidation
520 reactions via combination of photocatalytic water oxidation and enzymatic
521 oxyfunctionalizations. Nat Catal 1:55-62.

522 9. Molina-Espeja P, Garcia-Ruiz E, Gonzalez-Perez D, Ullrich R, Hofrichter M,
523 Alcalde M. 2014. Directed evolution of unspecific peroxygenase from *Agrocybe*
524 *aegerita*. Appl Environ Microb 80:3496-3507.

525 10. Molina-Espeja P, Ma S, Mate DM, Ludwig R, Alcalde M. 2015. Tandem-yeast
526 expression system for engineering and producing unspecific peroxygenase.
527 Enz Microb Tech 73-74:29-23.

528 11. Molina-Espeja P, Cañellas M, Plou FJ, Hofrichter M, Lucas F, Guallar V,
529 Alcalde M. 2016. Synthesis of 1-naphthol by a natural unspecific peroxygenase
530 engineered by directed evolution. ChemBioChem 17:341-349.

12. Molina-Espeja P, Gomez de Santos P, Alcalde M. 2017. Directed evolution of unspecific peroxygenase, p 127-143. *In* Alcalde M (ed), Directed Enzyme Evolution: Advances and Applications,Springer, Switzerland.

13. Mate DM, Palomino MA, Molina-Espeja P, Martin-Diaz J, Alcalde M. 2017. Modification of the peroxygenative: peroxidative activity ratio in the unspecific peroxygenase from *Agrocybe aegerita* by structure-guided evolution. Protein Eng Des Sel 30:189-196.

14. Gomez de Santos P, Cañellas M, Tieves F, Younes SHH, Molina-Espeja P, Hofrichter M, Hollmann F, Guallar V, Alcalde M. 2018. Selective synthesis of the human drug metabolite 5´-hydroxypropranolol by and evolved self-sufficient peroxygenase. ACS Catal. Submitted.

15. Goldsmith M, Tawfik DS. 2013. Enzyme engineering by targeted libraries. Methods Enzymol 523:257-283.

16. Mate DM, Gonzalez-Perez D, Mateljak I, Gomez de Santos P, Vicente AI, Alcalde M. 2016. The pocket manual of directed evolution: Tips and tricks, p 185-214. *In* Brahmachari G, Demain A, Adrio JL. (eds), Biotechnology of Microbial Enzymes: Production, Biocatalysis and Industrial Applications, Elsevier, Amsterdam.

17. Kaltenbach M, Tokuriki N. 2014. Generation of effective libraries by neutral drift. Methods Mol Biol 1179:69-81.

18. Peisajovich SG, Tawfik DS. 2007. Protein engineers turned evolutionists. Nat Methods 4:991-994.

19. Amitai G, Gupta RD, Tawfik DS. 2007. Latent evolutionary potentials under the neutral mutational drift of an enzyme. Hfsp J 1:67-78.

20. Bloom JD, Lu Z, Chen D, Raval A, Venturelli OS, Arnold FH. 2007. Evolution favors protein mutational robustness in sufficiently large. BMC Biol 5:29.

21. Bloom JD, Romero PA, Lu Z, Arnold FH. 2007. Neutral genetic drift can alter promiscuous protein functions, potentially aiding functional evolution. Biol Direct 2:17.

22. Bershtein S, Goldin K, Tawfik DS. 2008. Intense neutral drifts yield robust and evolvable consensus proteins. J Mol Biol 379:1029-1044.

23. Bershtein S, Tawfik DS. 2008. Ohno´s model revisited: measuring the frequency of potentially adaptive mutations under various mutational drifts. Mol Biol Evol 25:2311-2318.

24. Gupta RD, Tawfik DS. 2008. Directed enzyme evolution via small and effective neutral drift libraries. Nat Methods 5:939- 942.

25. Smith WS, Hale JR, Neylon C. 2011. Applying neutral drift to the directed molecular evolution of a β-glucuronidase into a β-galactosidase: Two different evolutionary pathways lead to the same variant. BMC Res Notes 4:138.

26. Tokuriki N, Jackson CJ, Afriat-Jurnou L, Wyganowski KT, Tang R, Tawfik DS. 2012. Diminishing returns and tradeoffs constrain the laboratory optimization of an enzyme. Nat. Commun 3:1257.

27. Keys TG, Fuchs HLS, Ehrit J, Alves J, Freiberger F, Gerardy-Schahn R. 2014. Engineering the product profile of a polysialyltransferases. Nat Chem Biol 10:437-442.

28. Zhao J, Kardashliev T, Joëlle Ruff A, Bocola M, Schwaneberg U. 2014. Lessons from diversity of directed evolution experiments by an analysis of 3,000 mutations. Biotechnol and Bioeng 111:2380-2389.

29. Bloom JD, Arnold FH. 2009. In the light of directed evolution: Pathways of adaptive protein evolution. Proc Natl Acad Sci USA 106:9995-10000.

30. Piontek K, Strittmatter E, Ullrich R, Gröbe G, Pecyna MJ, Kluge M, Scheibner K, Hofrichter M, Plattner DA. 2013. Structural basis of substrate conversion in a

583 new aromatic peroxygenase cytochrome P450 functionality with benefits. J Biol
584 Chem 288:34767-34776.

585 31. Gonzalez-Perez D, Garcia-Ruiz E, Alcalde M. 2012. *Saccharomyces*
586 *cerevisiae* in directed evolution: an efficient tool to improve
587 enzymes. Bioengineered 3:1-6.

588 32. Viña-Gonzalez J, Gonzalez-Perez D, Alcalde M. 2016. Directed evolution
589 method in *Saccharomyces cerevisiae*: Mutant library creation and
590 screening. Jove-J Vis Exp 110:e53761.

591 33. Ullrich R, Nüske J, Scheibner K, Spantzel J, Hofrichter M. 2004. Novel
592 haloperoxidase from the agaric basidiomycete *Agrocybe aegerita* oxidizes aryl
593 alcohols and aldehydes. Appl Environ Microbiol 70:4575–4581.

594 34. Anh DH, Ullrich R, Benndorf D, Svatoś A, Muck A, Hofrichter M. 2007. The
595 coprophilous mushroom *Coprinus radians* secretes a haloperoxidase that
596 catalyzes aromatic peroxygenation. Appl Environ Microbiol 73:5477–5485.

597 35. Gröbe G, Ullrich R, Pecyna MJ, Kapturska D, Friedrich S, Hofrichter M,
598 Scheibner K 2011. High-yield production of aromatic peroxygenase by the
599 agaric fungus *Marasmius rotula*. AMB Express 2011:1–31.

600 36. Kiebist J, Schmidtke KU, Zimmermann J, Kellner H, Jehmlich N, Ullrich R,
601 Zänder D, Hofrichter M, Scheibner K. 2017. A peroxygenase from *Chaetomium*
602 *globosum* catalyzes the selective oxygenation of testosterone. ChemBioChem
603 18:563-569.

604 37. Paradis E, Claude J, Strimmer K. 2004. APE: analyses of phylogenetics and
605 evolution in R language. Bioinformatics 20:289–290.

606 38. Gonzalez-Perez D, Alcalde M. 2018. The making of versatile peroxidase by
607 directed evolution. Biocat Biotransfor 36:1-11.

608 39. Siddiqui KS. 2017. Defying the activity-stability trade-off in enzyme entropy to
609 enhance activity and stability. Crit Rev Biotechnol. 37: 309-322.

FIGURE LEGENDS

Fig. 1. One-pot strategy for neutral drift and *in vivo* DNA shuffling. The epPCR library, with a mutational load of 1-3 mutation per Kb, was transformed in *S. cerevisiae* along with the linearized vector. To foster DNA shuffling and cloning *in vivo*, 50 bp overlapping stretches flanking each PCR product were included that are homologous to the ends of linearized vector. Clones with at least 45% of activity with respect to the parental PaDa-I were considered neutral, and their corresponding plasmids were isolated, mixed and used as the parental type for a new round of neutral drift/DNA shuffling. Squares, neutral mutations maintained; stars, new mutations.

Fig. 2. Neutral drift/DNA shuffling landscapes from generation 1 to 8. The activity of the clones is plotted in descending order, the solid line showing the activity of the parental PaDa-I and the dashed line represents the activity threshold with purged clones within the blue region. Clones satisfying the activity threshold were considered neutral and used as parental variants in the subsequent rounds: $\bar{m}_{nt}$, average nucleotide mutations; $\bar{m}_{aa}$, average amino acid mutations.

Fig. 3. Cladogram of neutrally evolved UPOs. The trees predicted by ClustalX2.1 and represented by Mega6 show the connections between 25 UPO homologues from generation 8 created by neutral drift and DNA shuffling: **(A)** cladogram constructed

637 from nucleotide substitutions (including silent mutations); **(B)** cladogram constructed
638 from amino acid substitutions (see also **Table S1** in supplemental material).

639 **Fig. 4. Mutations of the neutrally evolved UPOs.** Mutations of the 25 variants
640 extracted from generation 8 are highlighted in different colors and related to the clone
641 number (front and back perspectives). Enriched mutations appear in several mutants
642 (see **Table S1** in supplemental material). Mutations mapped in the *A. aegerita* UPO
643 crystal structure (PDB accession number 2YOR).

644 **Fig. 5. Palette of activities and stabilities of neutrally evolved UPOs.** Heat maps of
645 activities **(A)** and stabilities **(B)**, showing the improvement (in fold) relative to the
646 parental type of the 25 neutrally evolved UPO variants from generation 8. In both maps
647 the variants are hierarchically organized into dendrograms according to their activity
648 **(A)**, and their tolerance to temperature and co-solvents **(B)** using the R-studio program
649 and the package 'ape' to arrange in clusters the different variants (37). Activity and
650 stability measurements were made in triplicate from supernatant preparations as
651 described in Material and Methods.

652

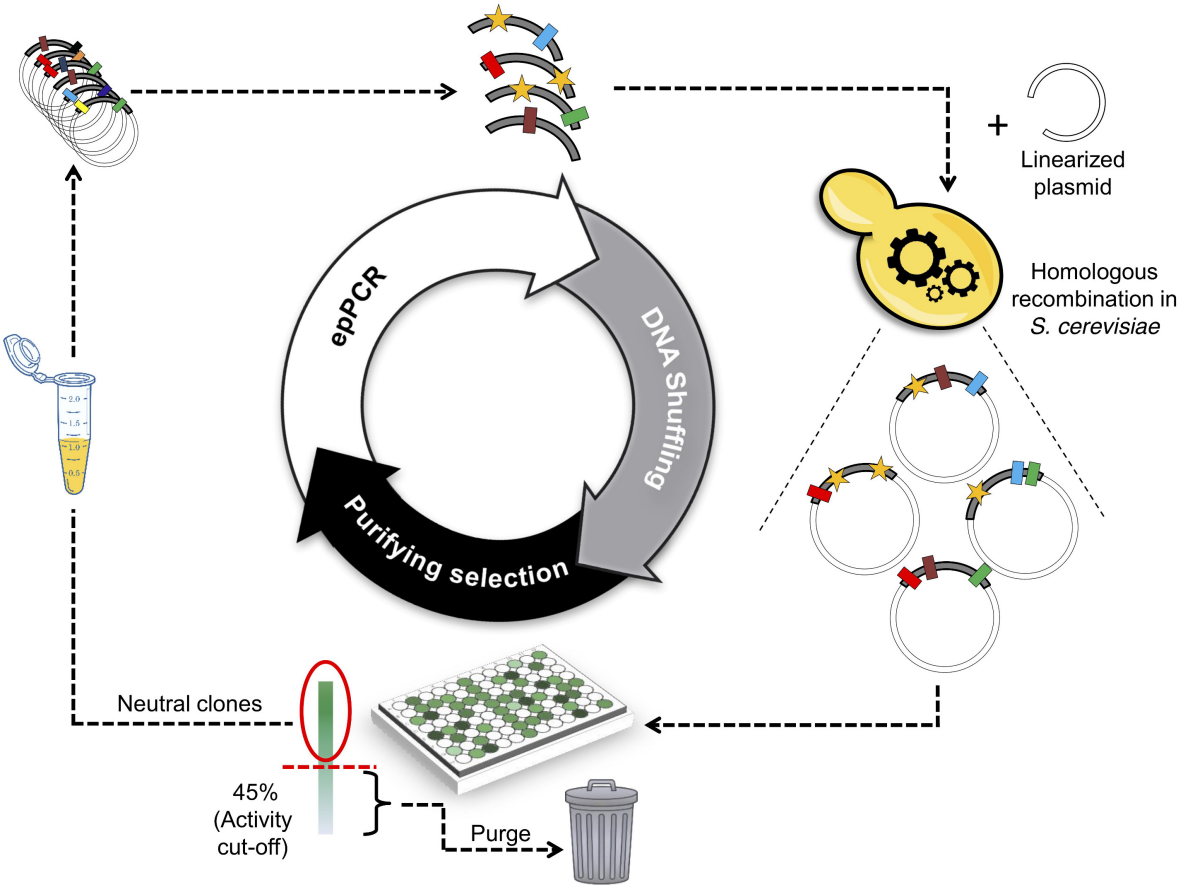

Fig. 1. One-pot strategy for neutral drift and *in vivo* DNA shuffling. The epPCR library, with a mutational load of 1-3 mutation per Kb, was transformed in *S. cerevisiae* along with the linearized vector. To foster DNA shuffling and cloning *in vivo*, 50 bp overlapping stretches flanking each PCR product were included that are homologous to the ends of linearized vector. Clones with at least 45 % of activity with respect to the parental PaDa-I were considered neutral, and their corresponding plasmids were isolated, mixed and used as the parental type for a new round of neutral drift/DNA shuffling. Squares, neutral mutations maintained; stars, new mutations.

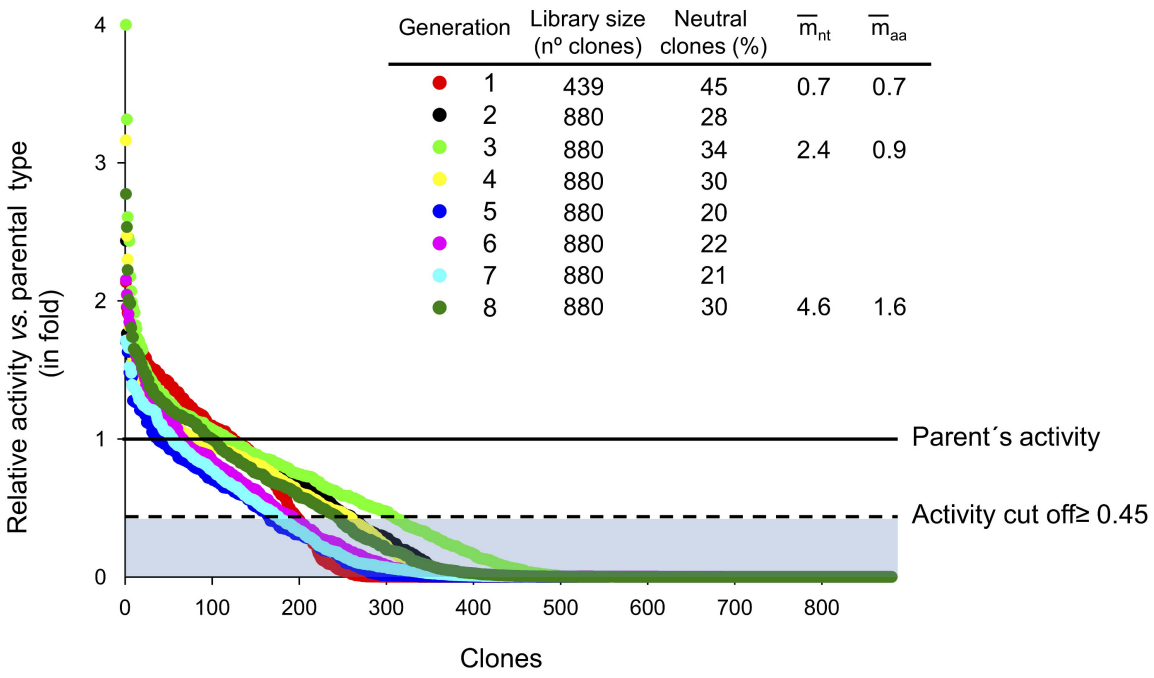

Fig 2. Neutral drift/DNA shuffling landscapes from generation 1 to 8. The activity of the clones is plotted in descending order, the solid line showing the activity of the parental PaDa-I and the dashed line represents the activity threshold with purged clones within the blue region. Clones satisfying the activity threshold were considered neutral and used as parental variants in the subsequent rounds: $\overline{m}_{nt}$, average nucleotide mutations; $\overline{m}_{aa}$, average amino acid mutations.

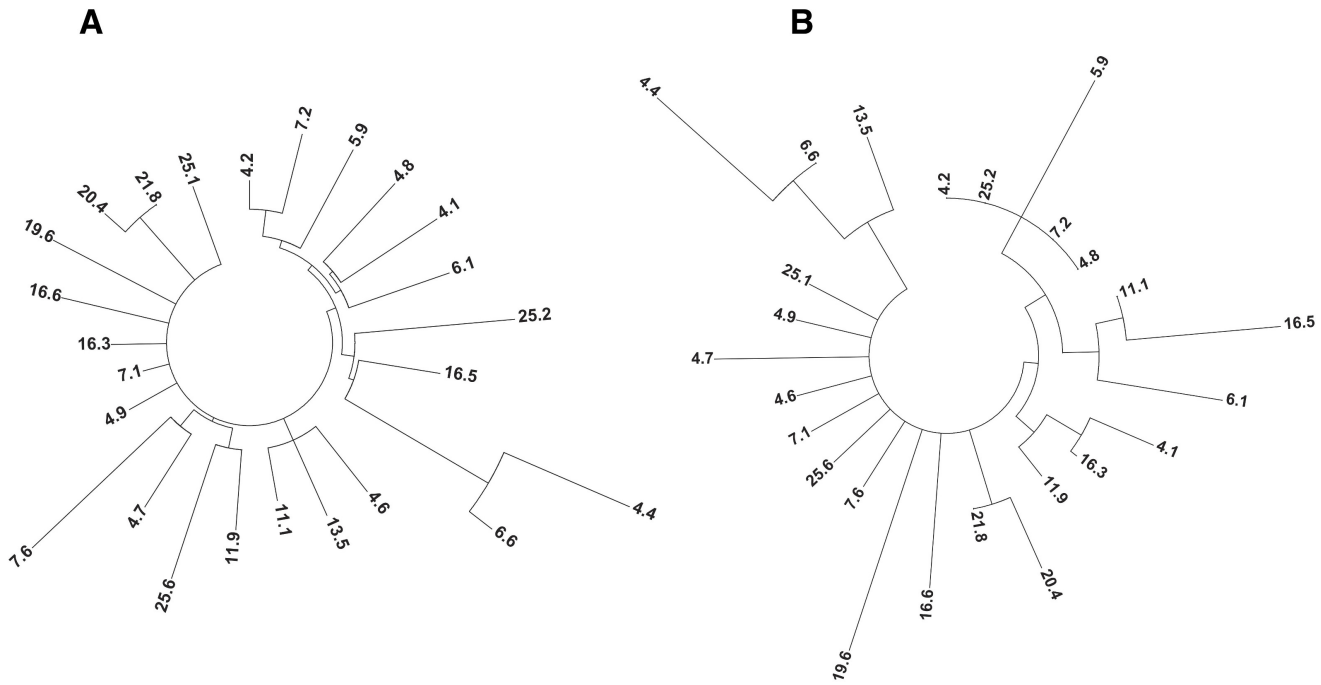

Fig. 3. Cladogram of neutrally evolved UPOs. The trees predicted by ClustalX2.1 and represented by Mega6 show the connections between 25 UPO homologues from generation 8 created by neutral drift and DNA shuffling: **(A)** cladogram constructed from nucleotide substitutions (including silent mutations); **(B)** cladogram constructed from amino acid substitutions (see also **Table S1** in supplemental material).

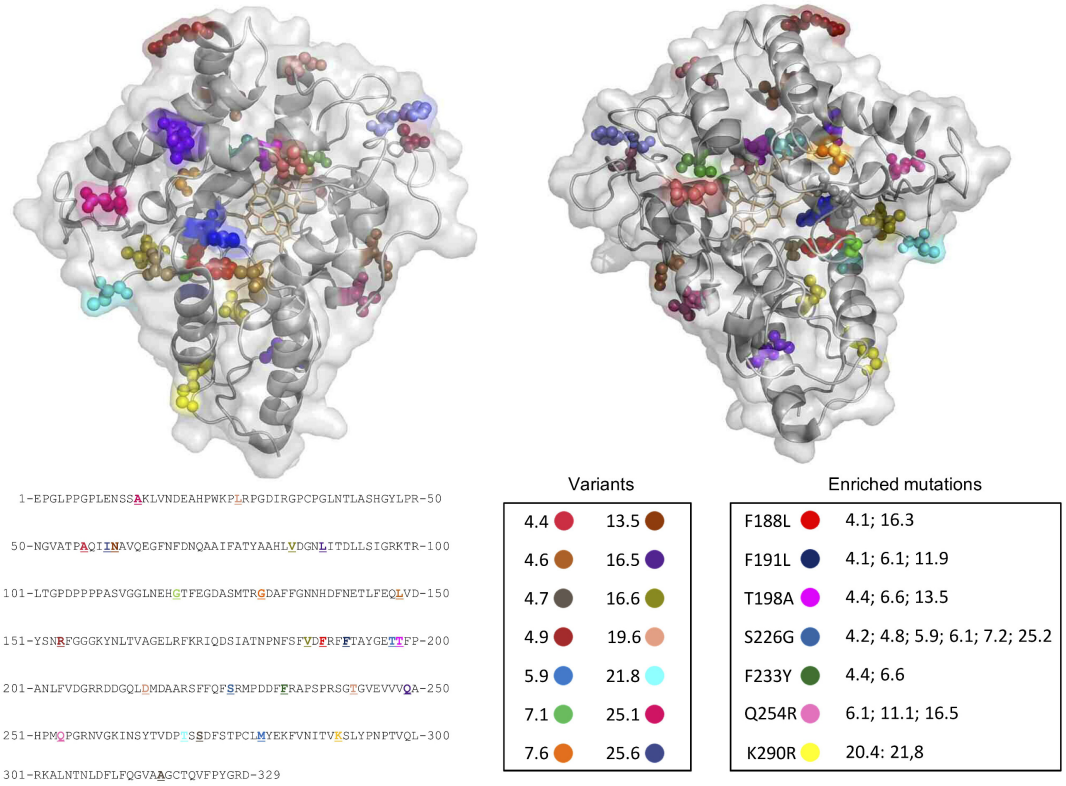

Fig. 4. Mutations of the neutrally evolved UPOs. Mutations of the 25 variants extracted from generation 8 are highlighted in different colors and related to the clone number (front and back perspectives). Enriched mutations appear in several mutants (see **Table S1** in supplemental material). Mutations mapped in the *A. aegerita* UPO crystal structure (PDB accession number 2YOR).

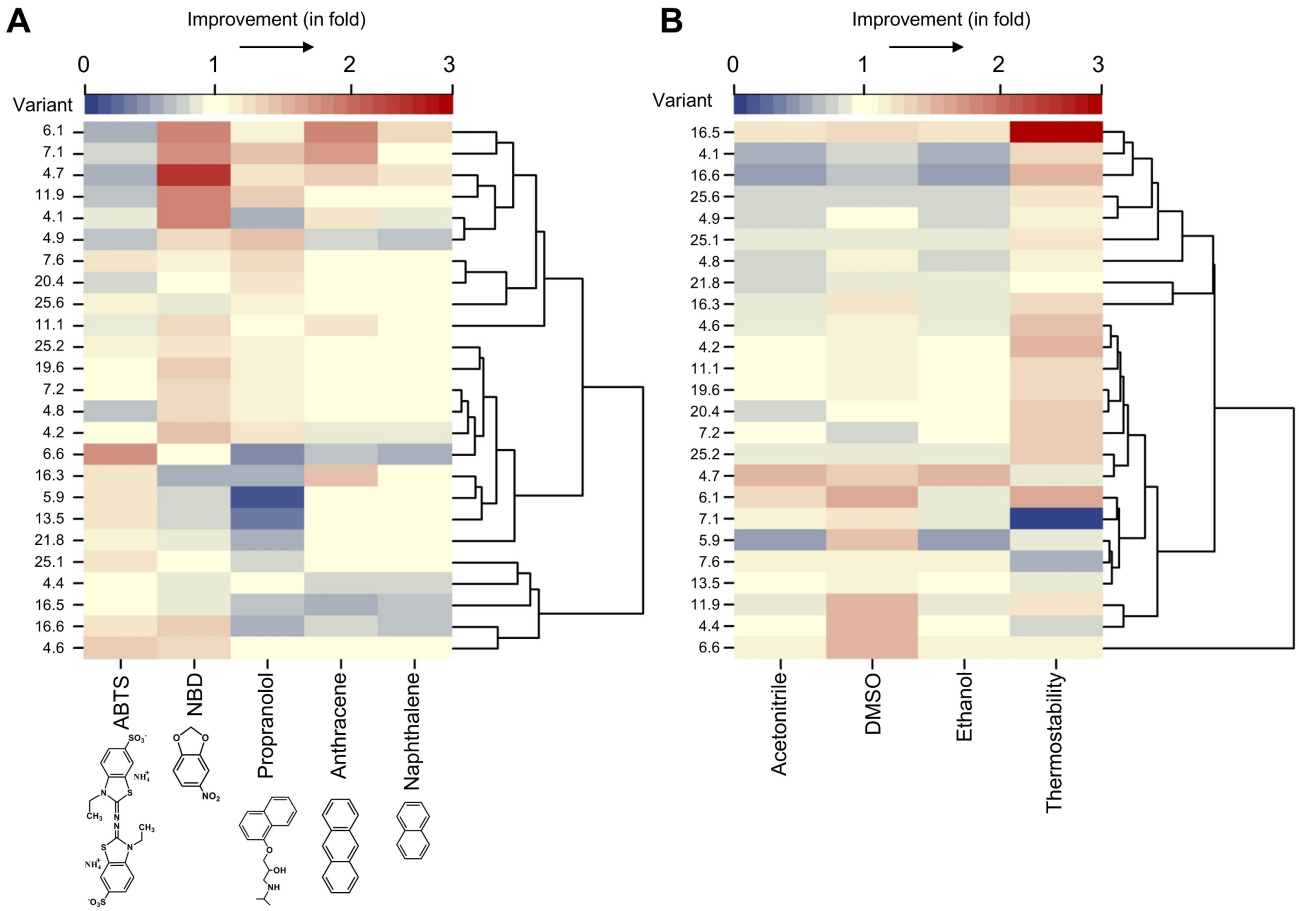

Fig. 5. Palette of activities and stabilities of neutrally evolved UPOs. Heat maps of activities **(A)** and stabilities **(B)**, showing the improvement (in fold) relative to the parental type of the 25 neutrally evolved UPO variants from generation 8. In both maps the variants are hierarchically organized into dendrograms according to their activity **(A)**, and their tolerance to temperature and co-solvents **(B)** using the R-studio program and the package 'ape' to arrange in clusters the different variants (37). Activity and stability measurements were made in triplicate from supernatant preparations as described in Material and Methods.

Table 1. Kinetic thermostability and activity in organic solvents[1].

		PaDa-I	16.5	6.1	7.1	4.7
Thermostability	$t_{1/2}$ (min)	8.7	43	16.6	2.9	8.7
ACN	C_{50} (%)	7.0	7.2	17.5	8.8	20.3
DMSO	C_{50} (%)	2.0	1.7	2.8	1.3	2.3
Ethanol	C_{50} (%)	1.0	1.0	1.0	1.0	1.0
Methanol	C_{50} (%)	8.4	8.8	9.6	7.8	9.7
Acetone	C_{50} (%)	10.0	11.6	13.2	8.1	13.1

[1]Values calculated from $t_{1/2}$ and C_{50} plots of Figure S5.

Table 2. Kinetic parameters of PaDa-I and neutrally evolved UPO variants

Substrate	Kinetic constant	PaDa-I	16.5	6.1	7.1	4.7
ABTS	K_m (mM)	0.067 ± 0.009	0.034 ± 0.003	0.052 ± 0.03	0.09 ± 0.02	0.09 ± 0.01
	k_{cat} (s^{-1})	670 ± 37	513 ± 12	370 ± 7	322 ± 43	246 ± 15
	k_{cat}/K_m (mM^{-1} s^{-1})	10,224 ± 1026	15,057 ± 2037	7,073 ± 285	3,504 ± 710	2,585 ± 244
DMP	K_m (mM)	0.088 ± 0.003	0.09 ± 0.01	0.29 ± 0.02	0.046 ± 0.006	0.21 ± 0.01
	k_{cat} (s^{-1})	167 ± 2	76 ± 8	162 ± 5	108 ± 4	264 ± 3
	k_{cat}/K_m (mM^{-1} s^{-1})	1,899 ± 51	777 ± 88	543 ± 27	2,396 ± 259	1,205 ± 25
NBD	K_m (mM)	0.66 ± 0.21	1.77 ± 0.51	0.65 ± 0.2	0.20 ± 0.03	0.19 ± 0.07
	k_{cat} (s^{-1})	303 ± 40	160 ± 26	170 ± 20	126 ± 4	131 ± 8
	k_{cat}/K_m (mM^{-1} s^{-1})	460 ± 108	90 ± 11	262 ± 50	629 ± 77	710 ± 222
Propranolol	K_m (mM)	2.1 ± 0.1	2.5 ± 0.2	5.7 ± 2.1	2.1 ± 0.2	0.61 ± 0.09
	k_{cat} (s^{-1})	186 ± 6	25 ± 1	255 ± 68	167 ± 10	81 ± 4
	k_{cat}/K_m (mM^{-1} s^{-1})	90 ± 3	10.0 ± 0.5	44 ± 5	78 ± 4	131 ± 13
Naphthalene	K_m (mM)	0.38 ± 0.09	0.49 ± 0.09	0.59 ± 0.07	0.19 ± 0.05	0.48 ± 0.05
	k_{cat} (s^{-1})	162 ± 14	119 ± 9	89 ± 4	97 ± 7	127 ± 5
	k_{cat}/K_m (mM^{-1} s^{-1})	421 ± 69	243 ± 31	150 ± 10	520 ± 116	264 ± 18
Veratryl alcohol	K_m (mM)	12 ± 0.8	10 ± 1	9 ± 3	7 ± 1	20 ± 3
	k_{cat} (s^{-1})	256 ± 8	141 ± 6	56 ± 7	107 ± 5	220 ± 22
	k_{cat}/K_m (mM^{-1} s^{-1})	21 ± 1	13 ± 0.8	6 ± 1	16 ± 2	11 ± 1
Benzyl alcohol	K_m (mM)	2.3 ± 0.3	2.5 ± 0.1	11 ± 2	2.3 ± 0.3	4.5 ± 0.3
	k_{cat} (s^{-1})	630 ± 26	506 ± 9	426 ± 50	282 ± 13	558 ± 17
	k_{cat}/K_m (mM^{-1} s^{-1})	271 ± 26	204 ± 8	39 ± 5	121 ± 13	124 ± 7

For each substrate, reactions were performed by triplicate following the increase of the absorption for ABTS (ε_{418}=36,000 M^{-1} cm^{-1}); NBD (ε_{425}=9,700 M^{-1} cm^{-1}); DMP (ε_{469}=27,500 M^{-1} cm^{-1}); propranolol (ε_{325}=1,996 M^{-1} cm^{-1}) naphthalene (ε_{303}=2,010 M^{-1} cm^{-1}); benzyl alcohol (ε_{280}=1,400 M^{-1} cm^{-1}) and veratryl alcohol (ε_{310}=9,300 M^{-1} cm^{-1}). Further details in the Material and Methods section.